

Integrated Hydrological and Hydraulic Modeling for Dam Breach Analysis: A Case Study of Mahadev Khola, Bhaktapur

Roshan Manandhar^{1*}, Santosh Bhattarai¹, Roma Thakurati¹, Surendra Maharjan², Sujan Shrestha^{1,3}

¹Institute of Engineering, Tribhuvan University, Lalitpur, Nepal

²Chapman University, California, USA

³Kathmandu Engineering College, Kathmandu, Nepal

**Corresponding author*

(Manuscript Received: 10/06/2024; Revised: 02/08/2024; Accepted: 26/08/2024)

ABSTRACT

Located in the Mahadev Khola region of Bhaktapur, Nepal, this study explores the essential functions of dams in water storage, hydropower, flood control, and resource management while emphasizing their vulnerability to catastrophic failures despite comprehensive engineering efforts. Historical failures, including those caused by overtopping, excessive inflow, and typhoon-induced breaches, highlight the necessity for robust safety measures. This research uses HEC-HMS for Probable Maximum Flood (PMF) modeling and HEC-RAS for simulating dam breaches for overtopping failure to generate precise outflow hydrographs and flood hazard maps. The model was calibrated using data from the highest observed flood on July 23, 2002, and validated with runoff data from July 9, 1998, achieving strong performance metrics: NSE of 0.86, R² of 0.85, and PBIAS of -6.12% for calibration, and NSE of 0.89, R² of 0.87, and PBIAS of -14.41% for validation. Our findings underscore the importance of detailed hydrological simulations, ongoing monitoring, and reinforcement to mitigate risks. Identifying significant risk zones, the study emphasizes the need for timely evacuations and safety protocols. Ultimately, this research demonstrates the effectiveness of HEC-RAS in enhancing dam safety assessments and improving community resilience against environmental uncertainties and evolving hydrological conditions.

Keywords: Probable maximum Flood (PMF); Probable Maximum Precipitation (PMP); HEC-RAS; HEC-HMS

1 INTRODUCTION

Dams, essential hydraulic structures constructed across streams or rivers, serve multiple purposes, including water storage, hydropower generation, flood control, and water resource management. Despite comprehensive engineering efforts and significant investments, dams can still fail, leading to catastrophic downstream impacts such as loss of life, habitat destruction, property damage, and economic losses. Historically, dam failures have occurred for various reasons: the South Fork Dam failed in 1889 due to overtopping, the Machhu II Dam disaster in 1979 resulted from excessive inflow and the Banqiao Dam collapsed in 1975 due to a typhoon-induced failure (Islam & Murakami, 2021). Notably, embankment dams, though generally more resilient, are still vulnerable to overtopping and internal erosion. Furthermore, dam breaks can also be triggered by high sediment loads and debris flow in rivers, underscoring the importance of studying landslides and sediment dynamics for dam safety (Maharjan et al., 2020; Rai et al., 2022; Thakurathi et al., 2021).

Addressing the critical gap in dam break analysis, which is often conducted without comprehensive hydrological studies, this study aims to: (1) calibrate and validate an event-based model to generate the Probable Maximum Flood (PMF) using HEC-HMS, (2) identify the outflow hydrograph from a dam breach, and (3) prepare a flood hazard map. Dam breach analysis, crucial for emergency planning, utilizes modeling tools like HEC-HMS to generate the PMF at the proposed dam location and HEC-RAS to predict inundation areas, depths, and flood peaks (Brunner et al., 2017). This study leverages HEC-RAS for simulating an embankment dam breach, providing critical insights for emergency action plans. Research indicates the effectiveness of these models in enhancing safety protocols and mitigating potential disaster impacts (Morris et al., 2019), aligning with historical data that highlight the necessity of robust dam safety measures (Palmieri et al., 2001).

2 Materials and Methodology

2.1 Study Area

Mahadev Khola, located in Changunarayan Municipality of Bhaktapur District, is a spring-fed perennial stream originating from Mahadev Pokhari in Nagarkot. The basin is flanked by dense forest on the left and a forest with shrubs on the right. The catchment area at the proposed dam site is 4.69 sq. km, characterized by high, stable slopes with medium to dense vegetation. Runoff is primarily from precipitation, with no snowmelt contribution, and the riverbed elevation is 1516 meters.

As a key water source for Bhaktapur district, Mahadev Khola's flow varies along its course. With the rapidly growing urban population, the existing water supply has become insufficient. To address this, the Department of Water Supply and Sewerage Management (DWSSM) is exploring alternatives for improved drinking water supply. Recently, the Water Supply and Sanitation Division Office (WSSDO) proposed the construction of a Water Impounding Dam (WID) to store monsoon rainwater and enhance the region's water supply infrastructure.

Mahadev Khola Dam is an embankment dam of height 50m proposed to satisfy the water demand of the people of Bhaktapur. Water from Mahadev Khola dam is used as an alternative source for drinking water purposes. The dam can store about 2.38 MCM of water which is huge as there is a residential area just downstream of the dam. Residential areas would be highly affected if the dam fails. Being an embankment dam, there is a high chance that the dam would fail from overtopping and piping mechanisms. Hence, Studying and analyzing the dam breach case is of primary importance to save not only the life of people, as well as property and other possible hazards. This study tries to study and analyses the impacts due to dam failure from overtopping and reduce the probable damages at the downstream.

Table 1: Salient Features of the Project

Name of the Project	Mahadev Khola Impounding Reservoir Project
District	Bhaktapur
Name of the River	Mahadev Khola
Purpose	Water Supply
Hydrology	
Catchment Area (up to Dam Site)	4.69 Km ²
Annual Precipitation	1893.43 mm

Average Monthly Flow	0.25 m ³ /s
Flood Discharge (1 in 20 years)	9.33 m ³ /s
Flood Discharge (1 in 10000 years)	71.06 m ³ /s
Probable Maximum Flood (PMF)	87.01 m ³ /s
Reservoir	
Full Supply Level (FSL)	1564 masl
Total Storage	2.38 million m ³
Dam	
Type of Dam	Earthen Embankment
Crest Elevation	1566 masl
Length of Crest	375 m
Width of Crest	8 m

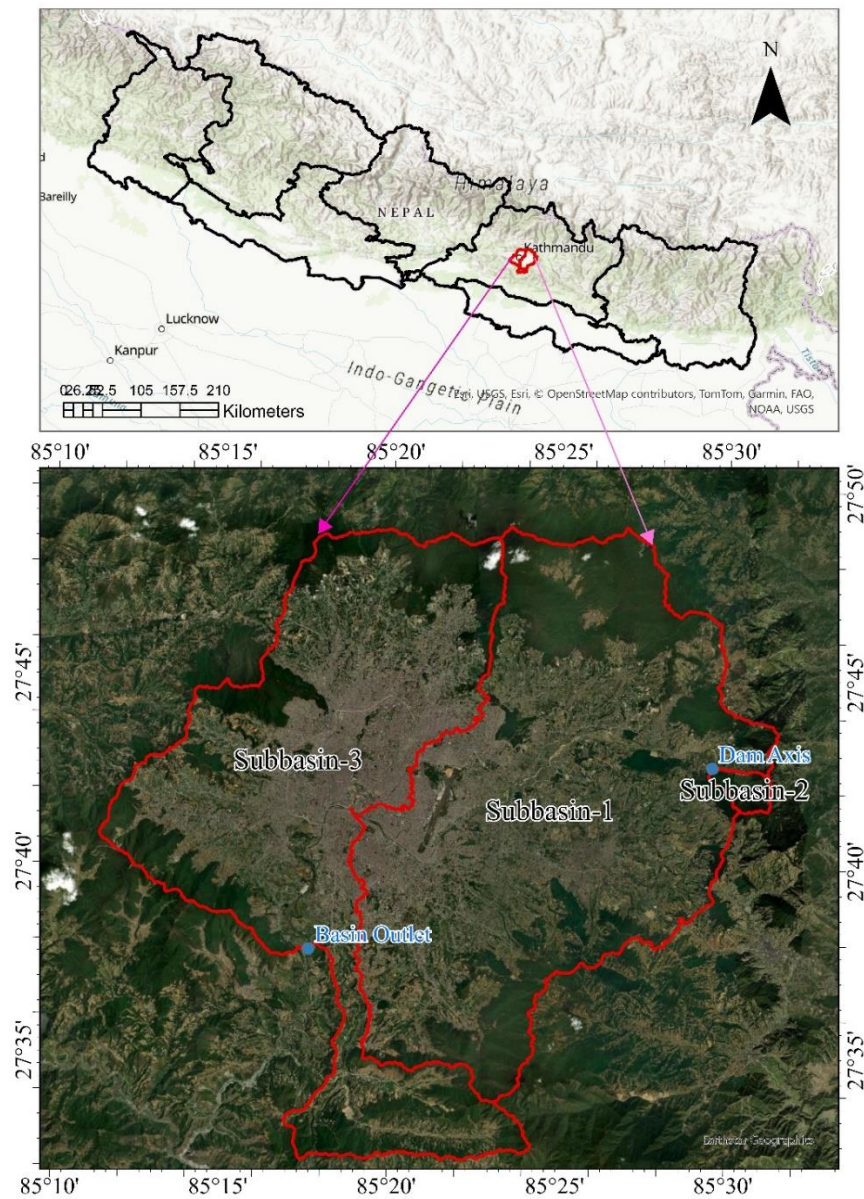


Figure 1: Geospatial Overview of the Study Region

2.2 Data Used

This study utilized spatial data, including the Digital Elevation Model (DEM), land cover maps, and geometric data for the dam, to investigate and analyze potential dam breaches. The Volume Elevation Curve for the dam reservoir was calculated from topographic survey data to ensure an accurate representation of the dam's storage phenomena, which is critical for dam breach analysis. Manning's roughness coefficient and percent impervious values were sourced from the HEC-RAS 2D manual for land cover types. Different ranges for dam breaching parameters were adopted according to guidelines from the Federal Energy Regulatory Commission (FERC) as specified in the HEC-RAS 2D manual.

Precipitation data were collected from meteorological and hydrological stations established by Nepal's Department of Hydrology and Meteorology (DHM) and additional climatic data, including minimum and maximum temperatures near the catchment area. The following tables list the meteorological and hydrological stations used for the study.

Table 2: Meteorological station name and number for the study

S. N	Station No.	Meteorological Station	S. N	Station No.	Meteorological Station
1	1074	Sundarijal	10	1059	Changunarayan
2	1071	Budanilkanta	11	1052	Bhaktapur
3	1035	Sakhu	12	1073	Khokana
4	1043	Nagarkot	13	1075	Lele
5	1049	Khopasi	14	1015	Thankot
6	1022	Godawari	15	1007	Kakani
7	1060	Chapagaun	16	1039	Panipokhari
8	1029	Khumaltar	17	1038	Dhunibesi
9	1030	Kathmandu Airport			

Table 3: Hydrological station name and number for the study

S. N	Station No.	Hydrological Station
1	550.05	Khokana Station

The Land Use and Land Cover (LULC) map was incorporated into the analysis. To provide a comprehensive elevation range, DEM data were sourced from ALOS PALSAR (<https://search.asf.alaska.edu/#/?zoom=3.000¢er=-97.494,39.673>) with a resolution of 12.5 m x 12.5 m, while land use classification data were obtained from ICIMOD 2019 (<http://rds.icimod.org/DatasetMasters/BulkDownload/1972729>) at a resolution of 30 m x 30 m. Building shapefiles were acquired from Open Street Maps (https://data.humdata.org/dataset/hotosm_npl_buildings?). The dam's geometric data include a maximum height of 50 meters above the foundation, a crest elevation of 1566 meters above sea level (masl), a crest length of 375 meters, and a crest width of 8 meters. The adopted values for dam breach parameters, as per FERC, include an average breach width of 50 meters, a horizontal component of breach side (H: V) of 1:1, a failure time of 0.5 hours, a weir coefficient of 1.45, a trigger failure elevation of 1566.1 masl, and an overtopping failure mode.

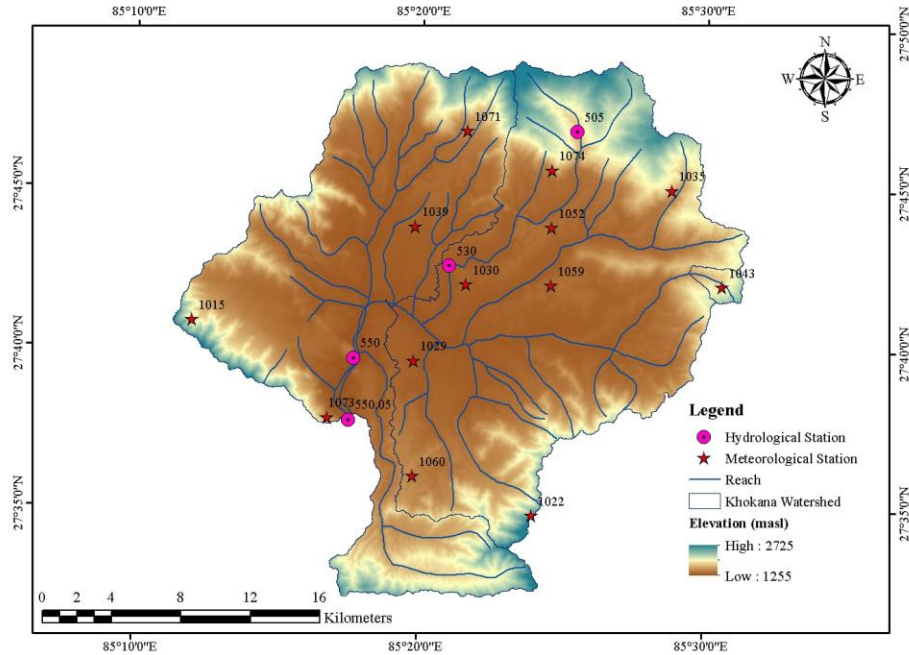


Figure 2: Watershed DEM for Khokana Station

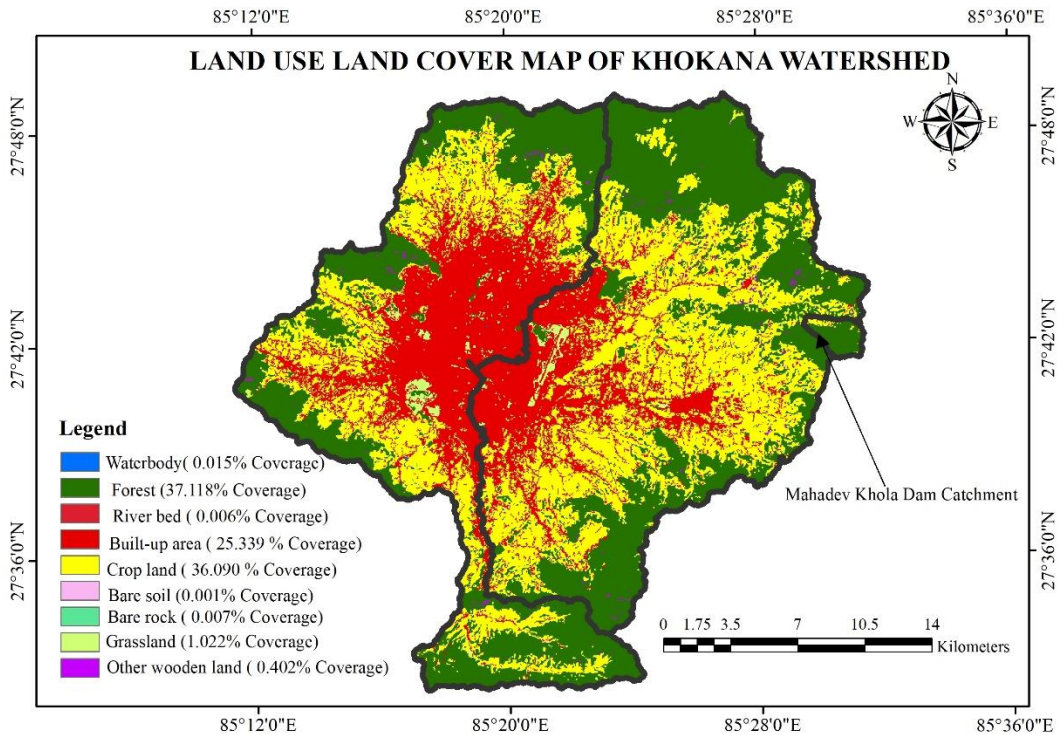


Figure 3: LULC Map of Khokana Watershed as per ICIMOD 2019

Figure 2 shows hydrological and meteorological stations, river reaches, and elevation variations, with elevations ranging from a minimum of 1255 meters to a maximum of 2725 meters above sea level. Figure 3 depicts the land use and land cover of the Khokana Watershed, highlighting various

categories. The highest land use coverage is forest at 37.118%, while the lowest is bare soil at 0.001%. Other land use categories include cropland (36.090%), built-up area (25.339%), grassland (1.022%), other wooded land (0.402%), water body (0.015%), bare rock (0.007%), and river bed (0.006%). The Mahadev Khola Dam catchment is also marked.

The Volume Elevation Curve illustrated in Figure 4 shows the relationship between the volume of water stored in the dam reservoir and the corresponding elevation of the water surface. As depicted, the curve begins at a lower elevation of approximately 1510 masl and shows a gradual increase in elevation as the volume increases. This upward-sloping curve highlights the nonlinear relationship between volume and elevation, where the elevation rises more rapidly with smaller volumes and more gradually as the volume increases. This relationship is crucial for understanding the reservoir's storage capacity, aiding in operational planning for flood management, water supply, and hydropower generation. Additionally, it is essential for dam safety analysis, as it helps predict water levels during various inflow conditions, thereby assessing the risk of overtopping and other potential failure scenarios. The description of all the data used is shown in Table 4.

Table 4: List of Spatial data acquired from different sources

Dataset	Data Type	Data Description / Processing	Resolution	Data Source
Terrain/DEM	Spatial grids	Digital Elevation Model	12.5 m x 12.5 m	ALOS PALSAR
Land Use	Spatial grids	Land use classification	30 m x 30 m	ICIMOD 2019
Building shape file				Open Street maps

Table 5: List of Geometric data for dam

Type	Earthen Dam
Maximum height above foundation	50 m
Crest Elevation	1566 masl
Length of Crest	375 m
Width of Crest	8 m

Table 6: Adopted value for dam breach parameters as per FERC

Dam Breach Parameters	Value
Average Breach Width	50 m
Horizontal Component of Breach Side (H) (H: V)	1:1
Failure Time (hrs.)	0.5
Weir Coefficient	1.45
Trigger Failure Elevation	1566.1 masl
Failure Mode	Overtopping

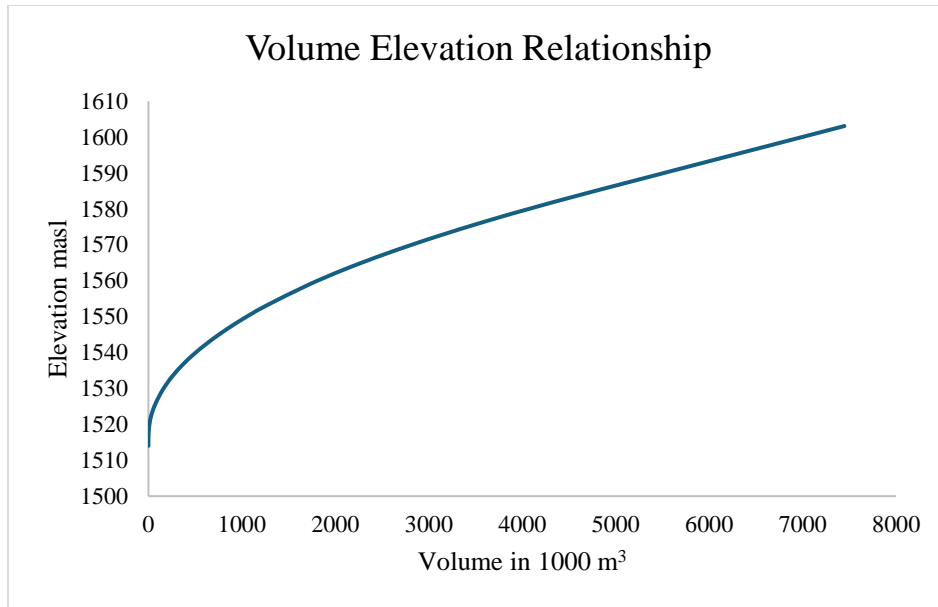


Figure 2: Volume Elevation Curve

2.3 METHODOLOGY

The systematic approach and methodology for investigating and analyzing dam breaches, particularly focusing on potential failure impacts, are crucial in hydraulic engineering and flood risk management. This process involves multiple levels designed to provide a comprehensive understanding of dam breach phenomena. A key component is PMF, essential for dam safety as it represents the highest possible flood event under extreme meteorological conditions. Using HEC-HMS, the PMF inflow hydrograph is simulated by gathering relevant meteorological and hydrological data, identifying extreme conditions, and specifying losses using hydrologic models like the SCS curve number method.

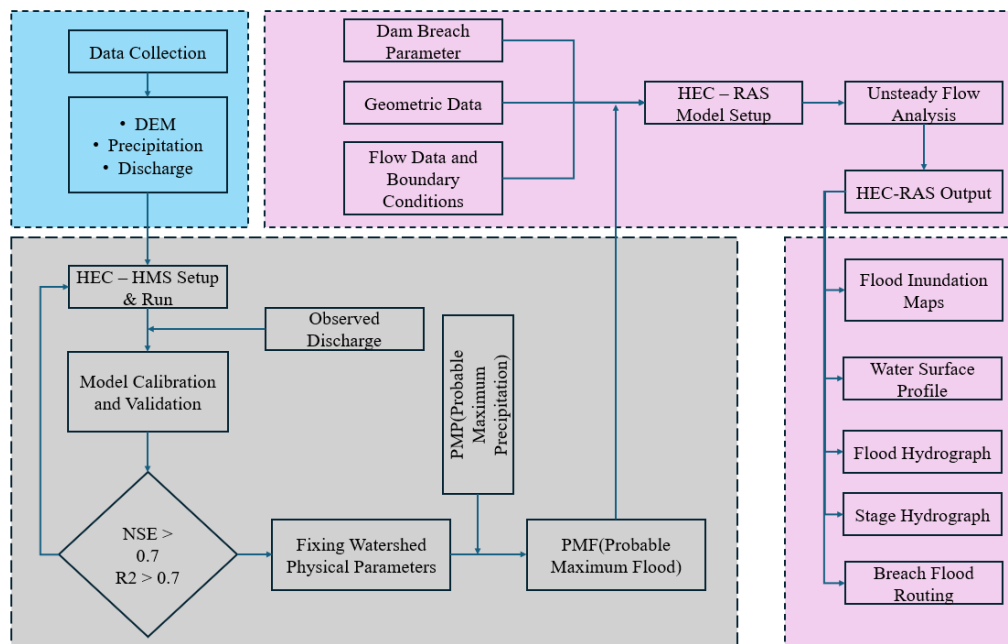


Figure 3: Working Methodology

This hydrograph is then input into HEC-RAS for further analysis. In this study, an overtopping failure case was considered. Data on dam geometry and storage areas were obtained, and connections between the reservoir and downstream areas were established. Breach parameters and boundary conditions were provided for unsteady flow analysis. The simulation in HEC-RAS produced flood hazard maps, arrival times, flow velocities, and breach hydrographs, offering critical insights into the potential impacts of dam failure.

2.3.1 Hydrological Modelling with Hec-Hms and Hydraulic Modelling with Hec-Ras

HEC-HMS (Hydrologic Engineering Center - Hydrologic Modeling System) is a software tool developed by the U.S. Army Corps of Engineers for hydrologic modeling, simulation, and watershed analysis. Studies have demonstrated the efficacy of the HEC-HMS model in simulating event-based runoff and flood hydrographs across various watersheds. (Reshma et al., 2013) applied the HEC-HMS model to the Walnut Gulch watershed in Arizona, USA, to simulate runoff for multiple rainfall events. Their research showed that the model performed satisfactorily, accurately simulating the runoff volume and peak flow times for different events, thus validating the model's robustness in flood prediction scenarios. Similarly, (Prabha & Tapas, 2020) utilized the HEC-HMS model for event-based rainfall-runoff modeling in the Ambabal sub-basin of the Godavari basin in India. Their findings highlighted the model's effectiveness in simulating flood hydrographs, achieving a high Nash-Sutcliffe efficiency, which indicates a strong agreement between the observed and simulated discharges. These studies collectively underscore the reliability of HEC-HMS for hydrological simulations and flood risk assessments.

While HEC-HMS is widely used for various hydrological analyses, including flood routing, it is not typically the first choice for PMF estimation. However, HEC-HMS can be powerful in estimating PMF, especially when combined with other tools and methodologies. PMF, defined as the maximum flood that can occur during extreme meteorological situations like continuous heavy precipitation over a catchment, is used as a worst-case scenario for assessing critical structures such as dams and spillways. Several studies have successfully utilized the HEC-HMS model to generate PMF hydrographs. For instance, (Sharma & Bhar, 2018) applied the HEC-HMS model in the Maithon watershed, demonstrating its effectiveness in simulating PMF using Probable Maximum Precipitation (PMP) data. Additionally, (Dahal et al., 2022) used HEC-HMS to model PMF in the Babai River Basin under various climate change scenarios, highlighting the model's robustness in flood risk assessment. Creating a precipitation-runoff model in HEC-HMS involves using the historically highest runoff events for calibration (July 2002) and the second highest for validation (July 1998) from the source described in Table 4. The PMF estimation process in HEC-HMS includes collecting meteorological and topographic data, creating hydrological models, and simulating extreme rainfall to obtain runoff and PMF inflow hydrographs using methods like the Soil Conservation Service (SCS) curve number or unit hydrograph method (*Manual on Estimation of Probable Maximum Precipitation (PMP)*, 2009).

The calibration process involved adjusting the model parameters to minimize the differences between the model's output and actual observation. Our model was calibrated for July 2002, which was identified as the month with the highest recorded rainfall within the available dataset. Similarly, model validation was performed by using another set of data for the month of July of the year 2003, the period of the second-highest rainfall within the available dataset. The calibrated parameters were used as input for the model validation to check for the goodness of fit (Althoff & Rodrigues, 2021).

The Nash-Sutcliffe Efficiency (NSE) and coefficient of correlation (R^2) were used to measure the goodness of fit and verify the model's calibration and validation.

$$NSE = 1 - \frac{\sum_{i=1}^n (Q_{obs_i} - Q_{sim_i})^2}{\sum_{i=1}^n (Q_{obs_i} - \bar{Q})^2}$$

where, NSE = Nash-Sutcliffe coefficient; Q_{sim} = simulated flow data (m³/s); Q_{obs} = Observed flow data (m³/s); \bar{Q} = Mean of observed flow (m³/s). R^2 ranges from 0 to 1, and it measures how collinearly the simulated data is aligned with the observed data, i.e., R^2 of 1 means simulated and observed are almost aligned in one straight line, implying that both data are almost equal. In comparison, R^2 of 0 means no correlation exists between the simulated and observed data. The following equation is used to compute R^2 :

$$R^2 = \left(\frac{\sum_{i=1}^n ((Q_{obs_i} - \bar{Q}_{obs_i}) \cdot (Q_{sim_i} - \bar{Q}_{sim_i}))}{\sqrt{\sum_{i=1}^n ((Q_{obs_i} - \bar{Q}_{obs_i})^2 \cdot \sum_{i=1}^n ((Q_{sim_i} - \bar{Q}_{sim_i})^2)}} \right)^2$$

$NSE > 0.50$ and $R^2 > 0.6$ are used as a criterion for satisfactory simulation in hydrological modeling, whereas $NSE > 0.75$ and $R^2 > 0.75$ are used as criteria for good simulation in hydrological modeling (Morris et al., 2019).

2.3.2 Estimation of PMP

Most procedures are based on a comprehensive meteorological analysis, while some are based on statistical analysis. Among the latter, the most widely used is Hershfield’s (Sarkar & Maity, 2020) A procedure based on the general equation has become one of the standard methods suggested by the World Meteorological Organization (WMO) for estimating PMP. It has the advantages of taking account of the actual historical data in the location of interest, expressing it in terms of statistical parameters, and being easy to use.

$$PMP = P_{max} + K \cdot S \dots\dots\dots (1)$$

Where:

- PMP = Probable Maximum Precipitation (in inches or mm)
- P_{max} = Maximum observed precipitation for a given duration (in inches or mm)
- K = Hershfield factor (frequency factor), which varies depending on the duration and location
- S = Standard deviation of annual maximum precipitation series

For K the following equation was used as

$$K_m = -5 \times 10^{-8} x^3 + 8 \times 10^{-5} x^2 - 0.052x + 19.794,$$

where x is the 24-hour mean annual maximum rainfall (mm). For our case, $x = 161.50$ mm
 $K_m = 13.48$.

2.3.3 Hydrodynamic Equations in Hec-Ras

The U.S. Army Corps of Engineers also developed HEC-RAS (River Analysis System), a software for hydraulic modeling of river systems, floodplain management, and dam breach modeling. HEC-RAS, valuable for modeling dam breaches in a two-dimensional context, assesses impacts on downstream areas and aids in emergency action plans (G. W. Brunner & Bonner, 1994). Initially, HEC-RAS could only conduct 1D dam breach analyses using the Saint-Venant equations, but it now supports 2D unsteady flow analysis using the diffusion wave equation (Goodell, 2014). This capability makes HEC-RAS a widely used tool in hydraulic engineering for dam breach scenarios. Studies like those by (Bharath et al., 2021; Prasad et al., 2024; Shahrin & Ros, 2020; Xiong, 2011) demonstrate HEC-RAS's effectiveness.

A different set of equations describes water flow in an open channel. In 1871, a French Engineer and mathematician, Adhemar Jean Claude Barre De Venant, described the full dynamics of rivers

and open channels, including the propagation of flood waves from dam breaches. These equations are a set of partial differential equations, one for the conservation of mass and another for the conservation of momentum.

$$\left(\frac{\partial Q}{\partial X}\right) + \frac{\partial(A+A_0)}{\partial T} - q = 0 \quad (\text{Continuity equation})$$

$$\left(\frac{\partial Q}{\partial T}\right) + \left\{\frac{\partial\left(\frac{Q^2}{A}\right)}{\partial X}\right\} + gA \left\{\left(\frac{\partial h}{\partial X}\right) + S_f + S_e\right\} = 0 \quad (\text{Momentum equation})$$

where, Q=discharge,

A=active flow area,

A₀= inactive storage area,

h=water surface elevation,

q=lateral inflow,

X=distance along the waterway, t=time,

S_f=friction slope,

S_c=expansion contraction slope and

g=gravitational acceleration.

3 Results and Discussion

3.1 Calibration and Validation of The Hec-Hms Model

Figure 6 shows the model's calibration and validation process, demonstrating robust performance in accurately simulating watershed behavior. Calibration was conducted using data from the highest observed flood on 23rd July 2002, with rainfall calculated using Thiessen polygons for the entire month of the watershed. Validation was performed with data from the second-highest observed runoff on 9th July 1998. The model's performance metrics were strong, with NSE, R², and PBIAS values of 0.86, 0.85, and -6.12% for calibration and 0.89, 0.87, and -14.41% for validation, indicating the model's reliability and accuracy. Additionally, the 95% confidence intervals shown in the scatter plots estimate the range within which the true regression line lies, highlighting the reliability and precision of the model's predictions. Key model parameters include an initial loss of 1 mm, a constant loss rate of 0.01 mm/hr, a time of concentration of 0.2 hours, a storage coefficient of 0.2 hours, an initial base flow discharge of 0.02 m³/s/Km², and a recession constant of 0.5. All these parameters were optimized with the goal of minimization of Mean Squared Errors. These parameters, combined with the strong correlation results and the narrow confidence intervals, underscore the model's robustness and reliability in simulating discharge for the watershed.

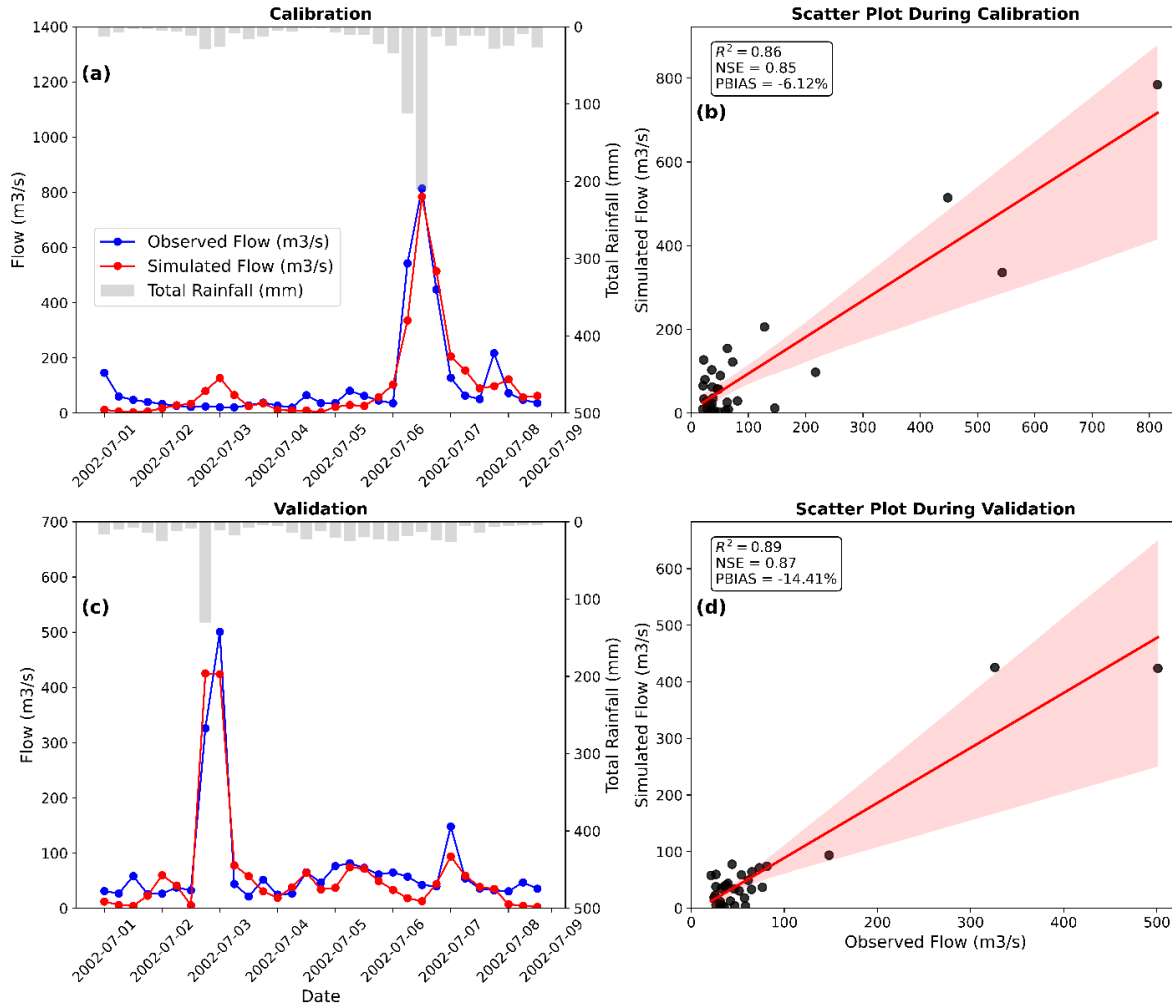


Figure 6: Calibration and Validation of Event-Based Model

3.2 Generation of PMF

After calibrating and validating the model at the basin outlet (as shown in Figure 1), it was employed to estimate PMF. PMP was calculated using the Hershfield method, as described in Section 2.3.1. The PMP, estimated to be approximately 360.70 mm with a coefficient of 13.48, was then utilized in HEC-HMS to calculate the PMF and generate the inflow hydrograph for a 24-hour period in the dam location catchment (as shown in Figure 1). The resulting hydrograph, which features a peak inflow of 87 m³/s and a base flow of approximately 4.4 m³/s during the PMF event (as depicted in Figure 7), was subsequently used in HEC-RAS to simulate the dam break analysis and create inundation maps.

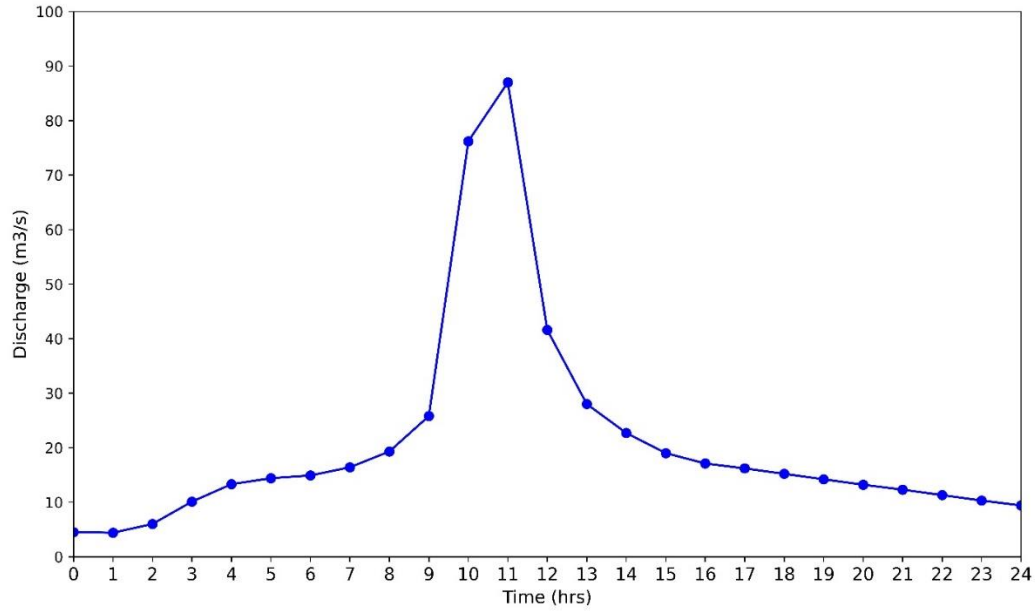


Figure 5: Generated PMF Hydrograph

3.3 Dam Breach Hydrograph and Inundation

The hydrograph begins with an initial release of water upon breach initiation, followed by a rapid increase as the breach widens. The peak flow represents the maximum discharge rate during the breach, capturing the intensity of the flood wave. Subsequently, as the breach closure mechanisms come into play, the hydrograph exhibits a gradual recession. Parameters such as breach geometry, material properties, and initial reservoir conditions significantly influence the shape and magnitude of the breach hydrograph. HEC-RAS allows for the customization of these parameters, enabling a detailed analysis tailored to the specific characteristics of the dam under study.

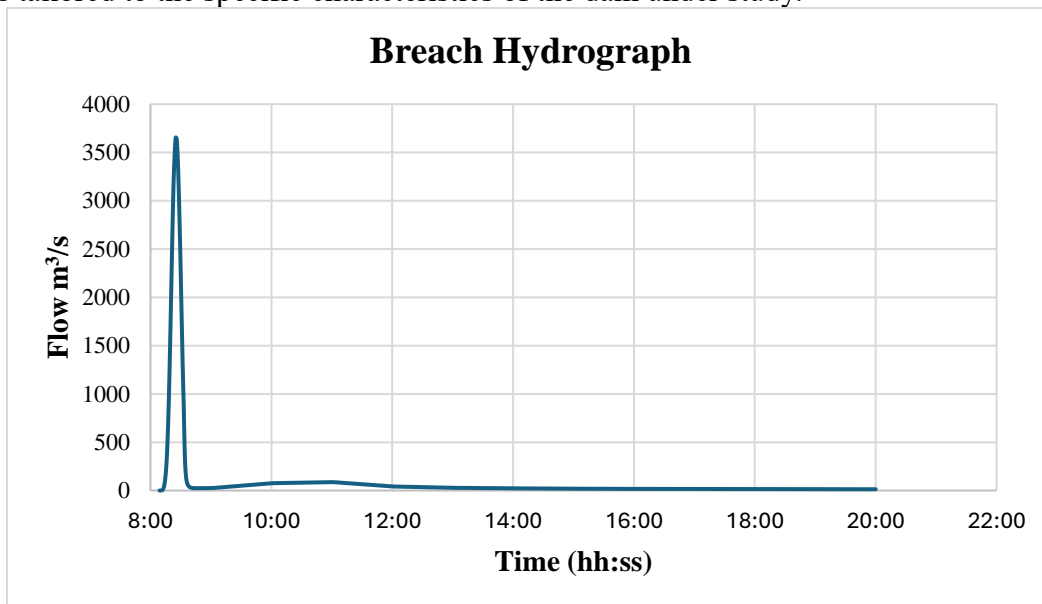


Figure 8: Breach Hydrograph at Dam

From the Figure 8, the peak flood of 3654 m³/s was seen at 08:25 hrs. while the dam breach initiation took place at 08:09, which means that it took 16 min to reach the peak flood from the breach initiation at the dam.

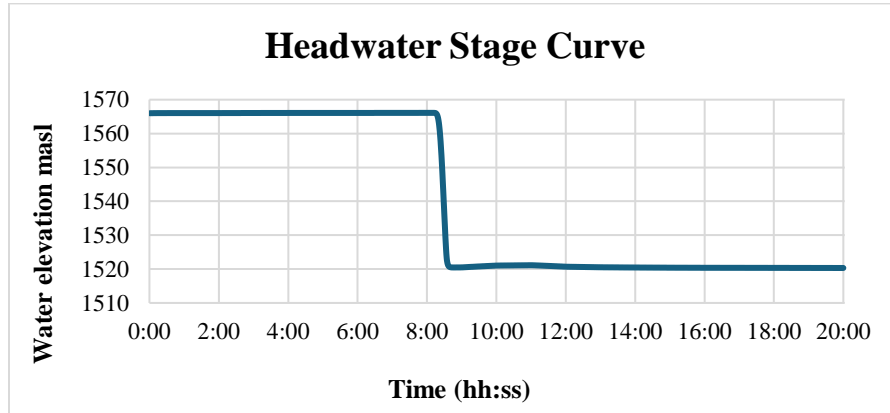


Figure 9: Headwater Stage Curve

The headwater stage curve plays a pivotal role in understanding hydraulic behavior during a dam breach. It is a graphical representation depicting the variation in water surface elevation in the reservoir (headwater) as a function of time during the breach process. The curve basically represents the water surface elevation upstream of the dam as a function of time during the event.

From Figure 9, the headwater stage is at 1566 masl and as the dam breach starts at 08:10, then the level starts to decrease as water starts releasing from the breach and after complete breaching of the dam, the water level stage can be seen at 1520.5, which shows the water at the reservoir after the full dam breach.

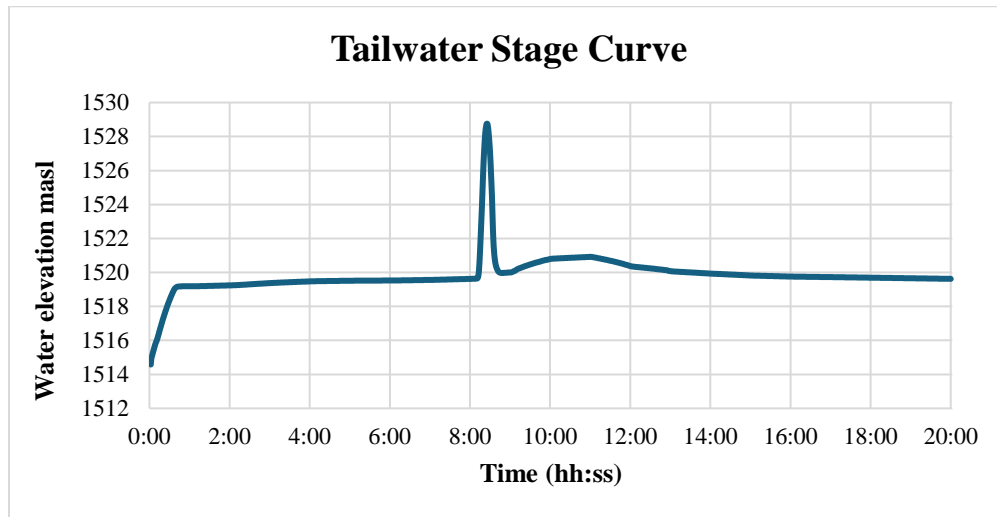


Figure 10: Tailwater Stage Curve

From Figure 10, it is seen that for the dry bat condition, the water initially rises and it is quite constant for some period that is up to 08:10. Then after the dam break occurs, the water level rises significantly and after peaking at 08:25, it eventually starts to decrease, which is also seen in the graph.

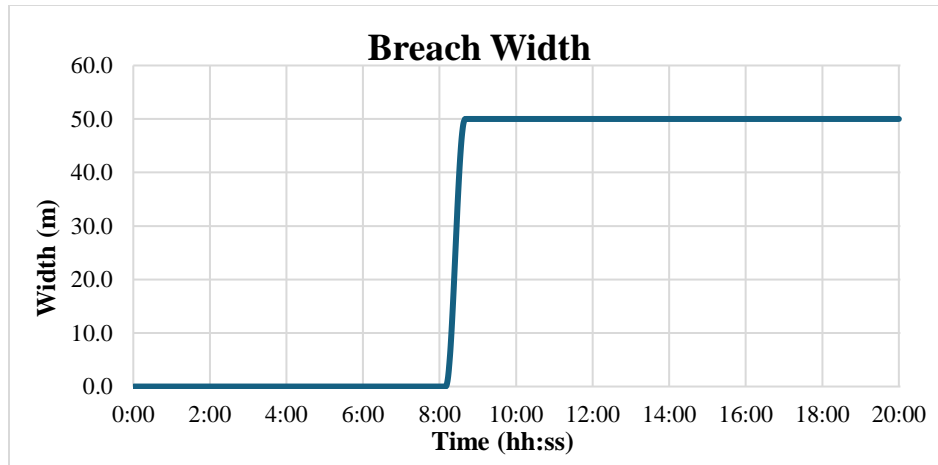


Figure 11: Breach width Curve

At the onset of the breach, characterized by PMF Events, the initial width is recorded at 0 m which means no breach of dam takes place. As the breach progresses chronologically, the chart captures the varying width of the breach, influenced by factors such as dam geometry, material properties, and hydraulic conditions.

Figure 11 shows the breach width is at 0 m initially up to 08:10 hrs. time at which dam breach initiates. Then, the breach width starts to increase rapidly and after completing dam breach, the breach width of 50m can be seen at from 08:25 hrs. which is the maximum breach assumed.

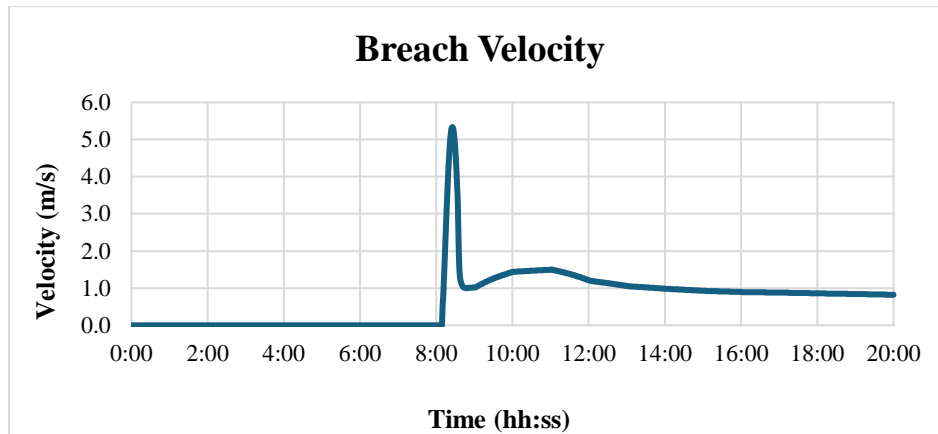


Figure 12: Breach velocity Curve

The initiation of the breach is marked by PMF event, leading to an initial breach velocity of 0 m/s at time zero means there is no flow escaping from the dam. As the breach progresses, the velocity undergoes dynamic changes, influenced by factors such as breach width, geometry, and hydraulic conditions. Figure 12 shows there is no flow from the dam up to 08:10 hrs., after the dam breach initiates, the velocity can be seen increasing and reached a peak of 5.33 m/s at 08:25 hrs. and then it starts decreasing as the time proceeds.

2D Unsteady flow simulation was performed in HEC-RAS for analyzing dam breach phenomena. Six different sections downstream of the dam were analyzed to study the flood hydrograph routing following an overtopping dam failure. The selected chainage points were located at 50 m, 850 m, 2100 m, 3900 m, 5500 m, and 6700 m downstream from the dam. The peak flood routing at these

river sections is illustrated in Figure 13, which shows the variation of the peak at different river cross-sections over time. The peak breach flow at the 50 m chainage was recorded at 3649.71 m³/s at 8:26:00 AM, which decreased to 2270.04 m³/s at the 6700 m chainage by 8:42:00 AM. A volume check was conducted to verify the accuracy of the peak flood data, ensuring that the volume at each cross-section remained consistent as per the conservation of mass principle. The volume at the breach was 3737.64 m³, while at the 6700 m chainage, the volume was 3590.11 m³, resulting in a minor error of 3.94%, likely attributable to software inaccuracies.

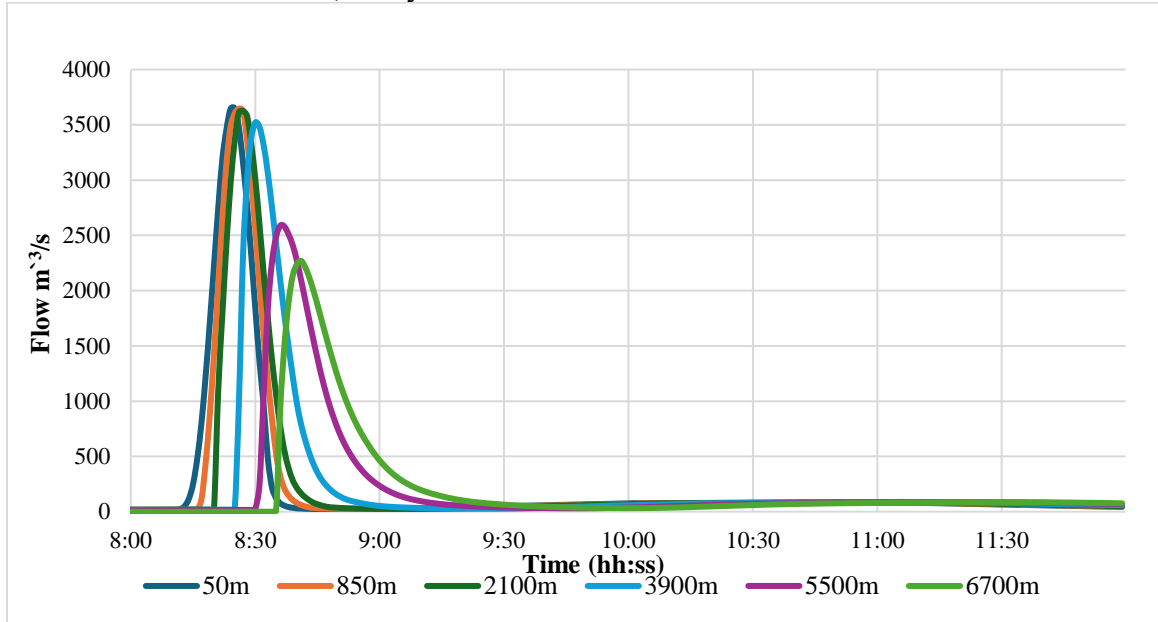


Figure 13: Breach Hydrograph along Different River Reach

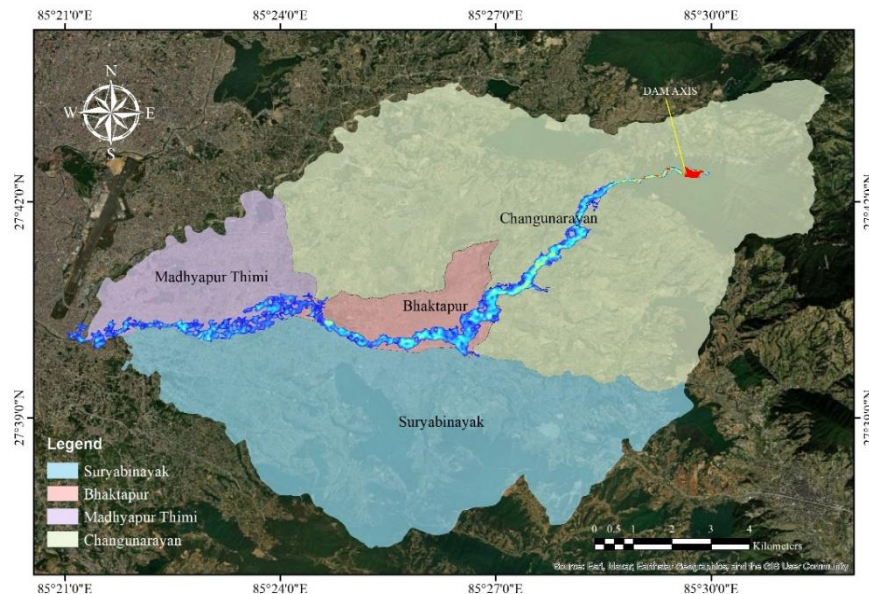


Figure 14: Area inundated with respect to a municipality

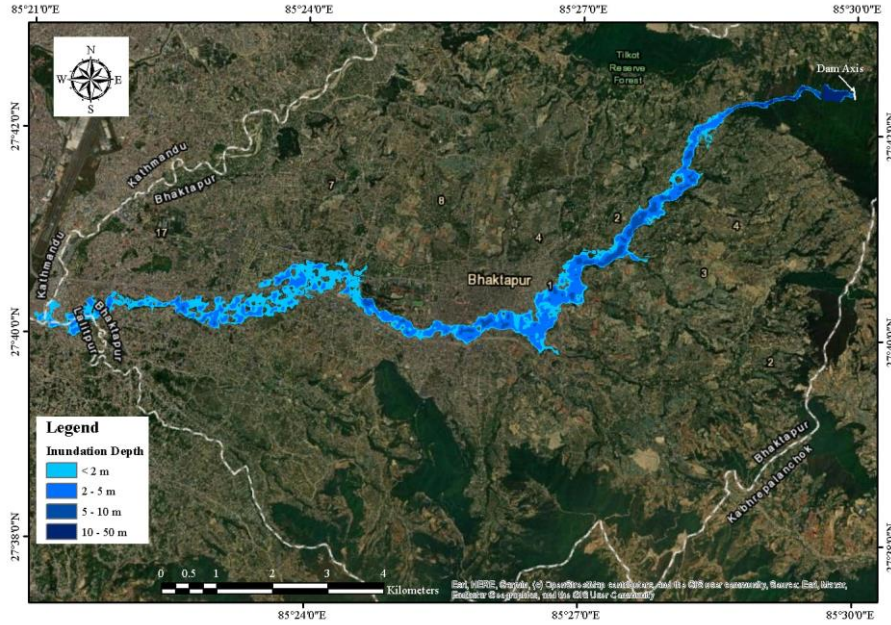


Figure 15: Flood Hazard map with important features after Dam Break

The total area inundated after the arrival of PMF into the storage area and the dam breach, including reservoir storage, was 3.70 square kilometers, as seen in Figure 14. The downstream region shows different residential areas. Within the downstream study area, four municipalities (Changunarayan, Bhaktapur, Suryabinayak & Madhyapur thimi) were inundated with inundation areas of 1.45, 1.54 km², 0.14 km² & 0.55 km², respectively.

Table 7 categorizes the number of buildings affected by varying flood depths in the event of a dam breach. Specifically, it identifies 1713 buildings that would be inundated by water depths ranging from 0 to 2 meters. Additionally, 1123 buildings fall within the 2 to 5-meter depth range, while 95 buildings are affected by depths of 5 to 10 meters. Only one building is impacted by water depths between 10 and 50 meters. Overall, a total of 2932 buildings are at risk across these different depth categories, highlighting the potential extent of infrastructural damage in the event of a flood.

Table 7: Potential Susceptible Building-to-Dam Break

S.N.	Depth	No of Buildings
1	0-2 m	1713
2	2-5 m	1123
3	5-10 m	95
4	10-50 m	1
	Total	2932

4 CONCLUSIONS

The comprehensive analysis of dam breaches using HEC-HMS and HEC-RAS has demonstrated its vital role in understanding and mitigating the risks associated with dam infrastructure. This study has underscored the importance of detailed hydraulic and hydrological simulations to identify potential failure points and the critical need for ongoing monitoring and reinforcement of dam systems. By integrating real-world data and various parameters, the research has highlighted the vulnerability of downstream communities and the necessity for robust emergency planning.

The findings revealed significant risk zones and emphasized the importance of timely evacuations and safety measures.

Furthermore, the application of HEC-RAS in this study bridges the gap between hydrology and hydraulics, enhancing our capability to assess dam vulnerabilities. This integration serves as a fundamental tool for ensuring the safety and resilience of communities in the face of environmental uncertainties and evolving hydrological patterns. In conclusion, this study not only strengthens our understanding of dam infrastructure risks but also promotes the implementation of effective mitigation strategies and emergency response plans.

REFERENCES

- [1] Althoff, D., & Rodrigues, L. N. (2021). Goodness-of-fit criteria for hydrological models: Model calibration and performance assessment. *Journal of Hydrology*, 600, 126674. <https://doi.org/10.1016/j.jhydrol.2021.126674>
- [2] Bharath, A., Shivapur, A. V., Hiremath, C. G., & Maddamsetty, R. (2021). Dam break analysis using HEC-RAS and HEC-GeoRAS: A case study of Hidkal dam, Karnataka state, India. *Environmental Challenges*, 5, 100401. <https://doi.org/10.1016/j.envc.2021.100401>
- [3] Brunner, G. W., & Bonner, V. R. (1994). *HEC River Analysis System (HEC-RAS)* [Report]. Hydrologic Engineering Center (U.S.). <https://erdc-library.erdc.dren.mil/jspui/handle/11681/32541>
- [4] Brunner, M. I., Viviroli, D., Sikorska, A. E., Vannier, O., Favre, A., & Seibert, J. (2017). Flood type specific construction of synthetic design hydrographs. *Water Resources Research*, 53(2), 1390–1406. <https://doi.org/10.1002/2016WR019535>
- [5] Dahal, A., Bhattarai, P. K., & Maharjan, S. (2022). *Analyzing the Future Flooding and Risk Assessment under CMIP6 Climate Projection Using HEC-HMS And HEC-RAS 2D Modelling of Babai River Basin*.
- [6] Goodell, J. D. (2014). *Search for the Standard Model Higgs boson in the $H \rightarrow WW \rightarrow l\nu q\bar{q}$ channel*.
- [7] Islam, K., & Murakami, S. (2021). Global-scale impact analysis of mine tailings dam failures: 1915–2020. *Global Environmental Change*, 70, 102361. <https://doi.org/10.1016/j.gloenvcha.2021.102361>
- [8] Maharjan, S., Yadav, A., & Shakya, N. M. (2020). *Sediment Simulation and Impact of Land Cover Changes using SWAT Model in Karnali Basin*.
- [9] *Manual on estimation of Probable Maximum Precipitation (PMP)*. (2009, March). <https://library.wmo.int/records/item/35708-manual-on-estimation-of-probable-maximum-precipitation-pmp?offset=7>
- [10] Morris, C. R., Stewardson, M. J., Finlayson, B. L., & Godden, L. C. (2019). Managing Cumulative Effects of Farm Dams in Southeastern Australia. *Journal of Water Resources Planning and Management*, 145(3), 05019003. [https://doi.org/10.1061/\(ASCE\)WR.1943-5452.0001041](https://doi.org/10.1061/(ASCE)WR.1943-5452.0001041)
- [11] Palmieri, A., Shah, F., & Dinar, A. (2001). Economics of reservoir sedimentation and sustainable management of dams. *Journal of Environmental Management*, 61(2), 149–163. <https://doi.org/10.1006/jema.2000.0392>
- [12] Prabha, J. A., & Tapas, M. R. (2020). *Event-Based Rainfall-Runoff Modeling Using HEC-HMS*.

- [13] Prasad, B., Tiwari, H. L., & Gupta, S. (2024). Dam Break Flood Inundation Mapping of Umrar Dam Using HEC-RAS. In P. V. Timbadiya, P. L. Patel, V. P. Singh, & V. L. Manekar (Eds.), *Flood Forecasting and Hydraulic Structures* (pp. 169–181). Springer Nature. https://doi.org/10.1007/978-981-99-1890-4_13
- [14] Rai, M. K., Maharjan, S., & Dahal, R. K. (2022). Landslide Susceptibility Assessment Using GIS-Based Weights-of-Evidence Model in the Khimti Khola Watershed, Eastern Nepal. *Bulletin of the Department of Geology*, 23, 35–51. <https://doi.org/10.3126/bdg.v23i1.64776>
- [15] Reshma, T., Venkata Reddy, K., & Deva, P. (2013). Simulation of Event Based Runoff Using HEC-HMS Model for an Experimental Watershed. *International Journal of Hydraulic Engineering*.
- [16] Sarkar, S., & Maity, R. (2020). Estimation of Probable Maximum Precipitation in the context of climate change. *MethodsX*, 7, 100904. <https://doi.org/10.1016/j.mex.2020.100904>
- [17] Shahrim, M. F., & Ros, F. C. (2020). Dam Break Analysis of Temenggor Dam Using HEC-RAS. *IOP Conference Series: Earth and Environmental Science*, 479(1), 012041. <https://doi.org/10.1088/1755-1315/479/1/012041>
- [18] Sharma, B., & Bhar, K. K. (2018). *Assessment of Probable Maximum Flood (PMF) using Hydrologic Model for Probable Maximum Precipitation in Maithon Watershed*.
- [19] Thakurathi, R., Maharjan, S., Ghimire, B. J., & Pandey, V. P. (2021). *Landslide Susceptibility Mapping of Khimti Watershed, Nepal*.
- [19] Xiong, Y. (2011). A Dam Break Analysis Using HEC-RAS. *Journal of Water Resource and Protection*, 03(06), 370–379. <https://doi.org/10.4236/jwarp.2011.36047>